

Reducing the complexity of finite-temperature auxiliary-field quantum Monte Carlo

C. N. Gilbreth^{a,1}, S. Jensen^b, Y. Alhassid^b

^a*Institute for Nuclear Theory, Box 351550, University of Washington, Seattle, WA 98195*

^b*Center for Theoretical Physics, Sloane Physics Laboratory, Yale University, New Haven, CT 06520*

Abstract

The auxiliary-field quantum Monte Carlo (AFMC) method is a powerful and widely used technique for ground-state and finite-temperature simulations of quantum many-body systems. We introduce several algorithmic improvements for finite-temperature AFMC calculations of dilute fermionic systems that reduce the computational complexity of most parts of the algorithm. This is principally achieved by reducing the number of single-particle states that contribute at each configuration of the auxiliary fields to a number that is of the order of the number of fermions. Our methods are applicable for both the canonical and grand-canonical ensembles. We demonstrate the reduced computational complexity of the methods for the homogeneous unitary Fermi gas.

1. Introduction

Strongly interacting quantum many-body systems of fermions are ubiquitous in condensed-matter physics, nuclear physics, cold atom physics, and quantum chemistry. Numerous theoretical approaches to their description exist, such as exact diagonalization, mean-field theory and its extensions, diagrammatic methods, density matrix renormalization group and tensor network algorithms, and quantum Monte Carlo (QMC) methods. QMC in particular is appealing in that, for certain classes of problems, it enables calculations that account for all quantum correlations of the system with a systematically controllable error.

The main advantage of QMC is that it scales gently (as a low power) in the number N_s of single-particle states of the model space. While offering a dramatic improvement to the exponential scaling of exact diagonalization methods, it is computationally demanding and its practicality for larger values of N_s depends sensitively on the particular power-law scaling in N_s .

Here we describe several algorithmic improvements for the finite-temperature auxiliary-field quantum Monte Carlo (AFMC) method. Principally, we introduce a novel method to identify, for a given field configuration, a subspace of

¹Current address: 2102 N Walnut St. Apt 182, Ellensburg, WA 98926

mostly unoccupied single-particle states, which does not contribute to observables, and remove this subspace from the calculation. Normally, AFMC calculations scale as $O(N_s^3)$ when updating the auxiliary fields, and $O(N_s^3)$ or higher for the calculation of observables. Our method reduces this scaling in most parts of the algorithm by reducing the number of contributing single-particle states to a number N_{occ} which depends weakly on the number of particles N , and is usually of order N . This can enable otherwise impractical calculations, in particular in systems where $N_s \gg N$. We have applied this method to precision thermodynamic studies on the lattice of strongly interacting cold Fermi gases, including the pseudogap phenomenon [1, 2] and thermodynamic observables in the continuum limit [3]. Our novel method is applicable for both the canonical and grand-canonical ensembles. An extension of our method was recently described in Ref. [4].

The outline of this article is as follows. In Sec. 1, we briefly review the finite-temperature AFMC method for fermions, including a description of numerical stabilization and particle-number projection. In Sec. 2, we discuss the method of reducing the single-particle model space based on the QR decomposition of the single-particle propagator, and show how to use this to efficiently compute one-body observables in the grand-canonical and canonical ensembles. In Sec. 3, we discuss the method of updating the fields. In Sec. 4, we consider two-body observables and describe a method to compute them efficiently in the canonical ensemble. In Sec. 5, we present our conclusion and outlook.

1.1. AFMC method

The finite-temperature AFMC method [5–7] is based on the Hubbard-Stratonovich transformation [8, 9], in which the thermal propagator $e^{-\beta\hat{H}}$, where \hat{H} is the Hamiltonian and $\beta = 1/T$ is the inverse temperature, is expressed as a path integral of a one-body propagator $\hat{U}(\sigma)$ with a Gaussian weight $G(\sigma)$ over auxiliary fields σ :

$$e^{-\beta\hat{H}} = \int D[\sigma] G(\sigma) \hat{U}(\sigma).$$

The auxiliary fields σ are real-valued quantities dependent on imaginary time τ and other indices. The imaginary time between $\tau = 0$ and $\tau = \beta$ is usually discretized into $N_t + 1$ equally spaced times $\tau_k = k\Delta\beta$ ($k = 0, 1, \dots, N_t$) where $\Delta\beta = \beta/N_t$. The propagator $\hat{U}(\sigma)$ describes a one-body propagator of non-interacting particles moving in one-body external fields, and can be written as a product of propagators for each time step, $\hat{U}(\sigma) = \hat{U}_{N_t} \cdots \hat{U}_1$. In the following we will simply write $\hat{U}(\sigma) = \hat{U}$, omitting the explicit σ dependence.

The thermal expectation value of an observable \mathcal{O} is calculated from

$$\langle \hat{\mathcal{O}} \rangle = \frac{\text{Tr}(e^{-\beta\hat{H}} \hat{\mathcal{O}})}{\text{Tr}(e^{-\beta\hat{H}})} = \frac{\int D[\sigma] W(\sigma) \langle \hat{\mathcal{O}} \rangle_{\sigma} \Phi_{\sigma}}{\int D[\sigma] W(\sigma) \Phi_{\sigma}},$$

where $W(\sigma) = G(\sigma) |\text{Tr} \hat{U}|$ is a positive-definite weight function, $\langle \hat{\mathcal{O}} \rangle_{\sigma} = \text{Tr}(\hat{U} \hat{\mathcal{O}}) / \text{Tr} \hat{U}$ is the expectation value of \mathcal{O} in a given configuration σ of the auxiliary fields,

and $\Phi_\sigma = \text{Tr} \hat{U} / |\text{Tr} \hat{U}|$ is the Monte Carlo sign function. The traces can be grand-canonical, canonical, or involve projections onto other quantum numbers (e.g., angular momentum and parity). Because \hat{U} is a one-body propagator, the traces can be computed using matrix algebra in the single-particle space of dimension N_s , yielding a scaling of $O(N_s^3)$ for the grand-canonical ensemble. For example, if the system is represented on a discrete spatial lattice, $N_s \propto N_L^3$, where N_L is the number of lattice points in each linear dimension, and the computational time scales as $O(N_L^9)$. Projections usually increase the computational complexity of calculating the trace. In what follows, we will denote grand-canonical traces by Tr , and canonical traces for N particles by Tr_N . Matrix traces will be denoted by tr .

A set of auxiliary fields σ_i are sampled stochastically according to $W(\sigma)$ and the expectation value of an observable \mathcal{O} is estimated from

$$\langle \hat{\mathcal{O}} \rangle \approx \frac{\sum_i \langle \hat{\mathcal{O}} \rangle_{\sigma_i} \Phi_{\sigma_i}}{\sum_i \Phi_{\sigma_i}}.$$

Various algorithms can be used (Metropolis-Hastings, Hybrid Monte Carlo, etc.) [10, 11] to sample the fields. For more details of the AFMC method, see Refs. [5, 7].

In the grand-canonical ensemble with chemical potential μ ,

$$\text{Tr}(\hat{U} e^{\beta \mu \hat{N}}) = \det(I + U e^{\beta \mu}), \quad (1)$$

where U is an $N_s \times N_s$ matrix representing the propagator \hat{U} in the space of single-particle states. For a one-body observable $\hat{\mathcal{O}} = \sum_{ij} \mathcal{O}_{ij} a_i^\dagger a_j$, we have

$$\langle \hat{\mathcal{O}} \rangle_\sigma = \frac{\text{Tr}(e^{\beta \mu \hat{N}} \hat{U} \hat{\mathcal{O}})}{\text{Tr}(e^{\beta \mu \hat{N}} \hat{U})} = \text{tr}(\mathcal{O} \rho), \quad (2)$$

where ρ is the one-body density matrix given by

$$\rho_{ij} = \langle a_j^\dagger a_i \rangle_\sigma = (I + e^{-\beta \mu} U^{-1})_{ij}^{-1}. \quad (3)$$

Computing (1) and (2) each typically requires $O(N_s^3)$ operations. This scaling can be reduced in principle by the method of pseudofermions, in which the determinant is computed by a stochastic sampling. This method is used extensively in lattice QCD calculations; however for nonrelativistic strongly interacting many-body systems, it does not necessarily result in a lower overall computational effort [10], and computing the determinant directly is far more common.

1.2. Particle-number projection

Several methods for canonical-ensemble calculations at finite temperature have been used or proposed [12–16]. We use an exact particle-number projection

obtained by applying a discrete Fourier transform of grand-canonical traces for each field configuration. This is accomplished with the projection operator [12]

$$\hat{P}_N = \frac{1}{N_s} \sum_{m=1}^{N_s} e^{i\varphi_m(\hat{N}-N)}, \quad (4)$$

where $\varphi_m = 2\pi m/N_s$ for $m = 1, \dots, N_s$. Inserting \hat{P}_N into the grand-canonical trace, we obtain the canonical partition function Z_N for a given field configuration

$$Z_N = \text{Tr}_N \hat{U} = \text{Tr}(\hat{P}_N \hat{U}) = \frac{e^{-\beta\mu_C N}}{N_s} \sum_{m=1}^{N_s} e^{-i\varphi_m N} \eta_m, \quad (5)$$

where $\eta_m \equiv \text{Tr}(e^{i\varphi_m \hat{N}} e^{\beta\mu_C \hat{N}} \hat{U}) = \det(I + e^{i\varphi_m} e^{\beta\mu_C} U)$. In Eq. (5) we have introduced a chemical potential μ_C for numerical stability, chosen for each sample such that $\text{Tr}(e^{\beta\mu_C \hat{N}} \hat{U} \hat{N}) / \text{Tr}(e^{\beta\mu_C \hat{N}} \hat{U}) = N$ ².

The canonical expectation value of an observable $\hat{\mathcal{O}}$ for N particles in a given configuration σ of the auxiliary fields can be computed from

$$\langle \hat{\mathcal{O}} \rangle_\sigma = \frac{\text{Tr}(\hat{P}_N \hat{U} \hat{\mathcal{O}})}{\text{Tr}(\hat{P}_N \hat{U})} = \frac{e^{-\beta\mu_C N}}{Z_N N_s} \sum_{m=1}^{N_s} e^{-i\varphi_m N} \langle \hat{\mathcal{O}} \rangle_\sigma^{(m)} \eta_m, \quad (6)$$

where Z_N is given by (5), and $\langle \hat{\mathcal{O}} \rangle_\sigma^{(m)} = \text{Tr}(e^{\beta\mu_C \hat{N}} e^{i\varphi_m \hat{N}} \hat{U} \hat{\mathcal{O}}) / \text{Tr}(\hat{U} e^{\beta\mu_C \hat{N}} e^{i\varphi_m \hat{N}})$.

In the case of the one-body density matrix, $\hat{\mathcal{O}} = a_i^\dagger a_j$ and $\langle a_i^\dagger a_j \rangle_\sigma^{(m)} = (I + e^{-\beta\mu_C - i\varphi_m} U^{-1})_{ji}^{-1}$. The thermal expectation value of two-body observables can be computed using Wick's theorem.

The calculation of projected observables in Eqs. (5), (6) can be accomplished in $O(N_s^3)$ operations by diagonalizing the matrix U [13, 17]. Given the eigenvalue decomposition $U = P \Lambda P^{-1}$, where $\Lambda_{ij} = \delta_{ij} \lambda_i$, we obtain

$$\eta_m = \prod_{k=1}^{N_s} (1 + e^{\beta\mu_C} e^{i\varphi_m} \lambda_k), \quad (7)$$

$$\rho_\alpha = \frac{e^{-\beta\mu_C N}}{Z_N N_s} \sum_{m=1}^{N_s} e^{-i\varphi_m N} \frac{\lambda_\alpha e^{\beta\mu_C} e^{i\varphi_m}}{1 + \lambda_\alpha e^{\beta\mu_C} e^{i\varphi_m}} \eta_m, \quad (8)$$

$$\rho_{ij} = \sum_{\alpha=1}^{N_s} P_{i\alpha} \rho_\alpha P_{\alpha j}^{-1}. \quad (9)$$

The $O(N_s^3)$ scaling of the diagonalization or calculation of the determinant can still be problematic for larger values of N_s . In Sec. 2 we discuss how to

²In exact arithmetic the formula (5) holds for any value of μ_C . However, it can be numerically unstable if μ_C is such that the average particle number in the grand-canonical ensemble is very different from N . In this case the desired N -particle trace will be a very small contribution to the expansion of the grand-canonical trace $\text{Tr}(e^{\beta\mu_C \hat{N}} \hat{U})$ in powers of $e^{\beta\mu_C}$, and will be difficult to extract numerically.

effectively reduce the dimension of the matrix U in order to further improve the scaling.

1.3. Numerical stabilization

AFMC simulations at large imaginary times involve long chains of matrix multiplications to compute $U = U_{N_\tau} \cdots U_1$, which can give rise to numerical instabilities when the matrices U become ill-conditioned [5, 18, 19]. To address this, one can accumulate a decomposition of U which separates out the important scales. One effective choice is the QDR decomposition $U = QDR$, where Q is unitary, D is diagonal with positive entries, and R is unit right-triangular. Although in principle a pivoted QR decomposition is preferable for obtaining this decomposition, in practice the QR decomposition without pivoting is highly accurate. A QR decomposition need not be done for every imaginary time τ_k , but can be done periodically, e.g., every K time slices (for instance $K = 16$). The numerical stabilization then requires $O([N_t/K]N_s^3)$ operations for each update of all auxiliary fields.

To diagonalize U , one cannot multiply out the factors QDR in this order without destroying the information contained in the smaller scales of D . Instead, one can diagonalize the similar matrix $S = DRQ$ and from this calculate number-projected observables. This procedure reduces the number of operations required for numerically stabilized canonical-ensemble calculations from $O(N_s^4)$ (without diagonalization) to $O(N_s^3)$ [17].

2. Model space truncation

In this section we introduce a novel method to reduce the dimension of the one-body propagator given the decomposition $U = QDR$ from N_s to N_{occ} , where N_{occ} is of the order of number of particles N . This reduces the computational complexity of both grand-canonical and canonical calculations to below $O(N_s^3)$ for all parts of the algorithm except the QR decomposition used for stabilization, and greatly speeds up calculations.

2.1. Omitting unoccupied states

In the decomposition $U = QDR$ for a given field configuration σ , the entries of the diagonal matrix D correspond roughly to the eigenvalues of U . Small eigenvalues of U correspond to mostly unoccupied single-particle states and contribute to observables proportionally to their magnitude. When their contribution is below a desired accuracy threshold, these states can be omitted from the model space, thereby reducing the dimension of the single-particle space in which traces are calculated.

In the following we will not assume the matrices Q and R to be unitary or right-triangular, respectively, but instead treat them as general complex matrices. This is necessary as the QR decomposition is not performed at every imaginary time step.

To properly truncate small scales which do not contribute to observables, a reference scale for the Fermi energy at the given field configuration is needed. In the grand-canonical ensemble, this is provided by the chemical potential μ . In the canonical ensemble, we determine an approximate chemical potential μ_D from the diagonal elements of D by numerically solving for μ_D in the equation

$$\sum_k \frac{d_k e^{\beta \mu_D}}{1 + d_k e^{\beta \mu_D}} = N,$$

where $D_{ij} = d_i \delta_{ij}$. In the following we will absorb the scale factor $e^{\beta \mu_D}$ or $e^{\beta \mu}$ into the elements of D , so that the Fermi energy is located at $d_k \approx 1$.

We separate out a certain number of the smallest diagonal values of D to reduce the rank of U . Sorting the entries of D in an appropriate order (see below), we write $D = D_{\text{occ}} + D_\varepsilon$, where $D_{\text{occ}} = \text{diag}(d_1, \dots, d_{N_{\text{occ}}}, 0, 0, \dots)$ and $D_\varepsilon = (0, 0, \dots, 0, d_{N_{\text{occ}}+1}, \dots, d_{N_s})$, and N_{occ} is the number of significantly occupied states. We then have

$$U = Q D_{\text{occ}} R + Q D_\varepsilon R = U_{\text{occ}} + E,$$

where $U_{\text{occ}} = Q D_{\text{occ}} R$ is the “occupied” part of U and $E = Q D_\varepsilon R$ is a small perturbation.

To determine N_{occ} , we choose it to be a small integer such that $\|E\| < \varepsilon$, where ε is a given small parameter and $\|\cdot\|$ is the Frobenius norm $\|E\| = \left(\sum_{ij} |E_{ij}|^2\right)^{1/2}$. This can be done with $O(N_s^2)$ operations using the upper bound

$$\|E\| \leq \|Q\| \|D_\varepsilon R\| = \|Q\| \left(\sum_{j=1}^{N_s} \sum_{k=N_{\text{occ}}+1}^{N_s} |d_k R_{kj}|^2 \right)^{1/2} < \varepsilon. \quad (10)$$

According to (10), the most natural sorting order of the d_k values is by the contributions $\sum_{i=1}^{N_s} |d_k R_{ki}|^2$ to $\|E\|$ rather than the d_k values themselves.

The number N_{occ} of significantly occupied states will depend on the number of particles N and the temperature T . For a given N and T , N_{occ} will increase gently with the total number N_s of single-particle states once N_s is sufficiently large to capture the relevant physics. Fig. 1 shows N_s and N_{occ} vs. lattice size (using a log-log scale) for the unitary Fermi gas at a temperature near the superfluid phase transition for the spin-balanced case with $N = 66$ particles (i.e., $N_\uparrow = N_\downarrow = 33$). In general, N_{occ} is of the order of the number of particles N .

We next permute the factors Q, D_{occ}, R to obtain

$$S_{\text{occ}} \equiv D_{\text{occ}} R Q = \left(\begin{array}{ccc|cc} X & X & X & X & X \\ X & X & X & X & X \\ x & x & x & x & x \\ 0 & 0 & 0 & 0 & 0 \\ 0 & 0 & 0 & 0 & 0 \end{array} \right)_{N_s \times N_s},$$

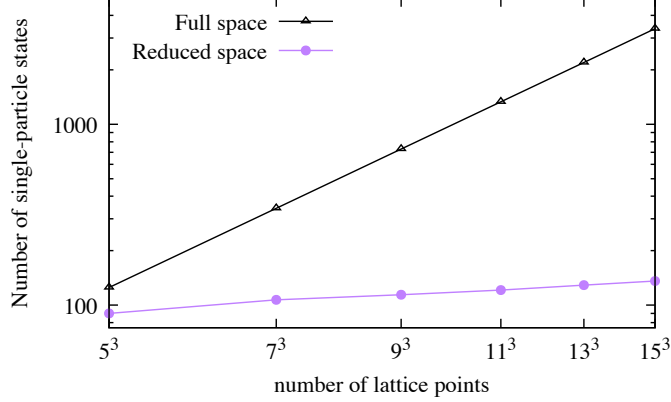


Figure 1: Dimensions N_s of the complete single-particle model space and N_{occ} of the reduced single-particle model space for the unitary Fermi gas near the superfluid phase transition as a function of the number of lattice points. The simulations were carried out for the spin-balanced case with $N = 66$ particles (Number projections were performed onto $N_{\uparrow} = N_{\downarrow} = 33$ particles), temperature $T = 0.14T_F$ (where T_F is the Fermi energy). To determine N_{occ} for the model space reduction we used $\varepsilon = 10^{-6}$. The number of states shown is for a single species, i.e., spin-up (\uparrow) or spin-down (\downarrow).

which is a similarity transformation $S_{\text{occ}} = Q^{-1}U_{\text{occ}}Q$. The boxed block in the equation above is an $N_{\text{occ}} \times N_{\text{occ}}$ matrix which we denote by \tilde{S} . Computing the matrix elements of \tilde{S} requires $O(N_s N_{\text{occ}}^2)$ operations.

The grand-canonical partition function that corresponds to the one-body propagator represented by the matrix U_{occ} can be computed from \tilde{S} as

$$Z = \det(I + \tilde{S}) , \quad (11)$$

which requires $O(N_{\text{occ}}^3)$ operations. To compute observables, we may assume that Q is unitary and R is unit right-triangular, since observable expectations are not computed during the field updates. The one-body density matrix ρ can then be computed from

$$\rho = Q [D_{\text{occ}} R Q (I + D_{\text{occ}} R Q)^{-1}] Q^\dagger , \quad (12)$$

which can be done in $O(N_s N_{\text{occ}}^2)$ operations.

To compute the partition function and observables in the canonical ensemble, we diagonalize \tilde{S} (using $O(N_{\text{occ}}^3)$ operations),

$$\tilde{S} = \tilde{P}_S \tilde{\Lambda} \tilde{P}_S^{-1} , \quad (13)$$

where $\tilde{\Lambda}_{ij} = \tilde{\lambda}_i \delta_{ij}$. The eigenvalues of S_{occ} and hence of $U_{\text{occ}} = Q S_{\text{occ}} Q^{-1}$ consist of the N_{occ} eigenvalues $\tilde{\lambda}_i$, along with $N_s - N_{\text{occ}}$ additional zero eigenvalues. Hence, the canonical partition function Z_N can be computed from Eqs. (5) and (7), in which N_s is replaced by N_{occ} and the eigenvalues λ_k are those of \tilde{S} .

To compute observables in the canonical ensemble, we need the transformation matrices for the eigenvalue decomposition³ of $U_{\text{occ}} = P\Lambda P^{-1}$. These can be obtained from \tilde{P}_S in (13) using $O(N_s N_{\text{occ}}^2)$ operations

$$P_{ij} = \sum_{k=1}^{N_{\text{occ}}} Q_{ik} \tilde{P}_{S,kj}, \quad i = 1, \dots, N_s, \quad j = 1, \dots, N_{\text{occ}} \quad (14)$$

$$P_{ij}^{-1} = \sum_{k=1}^{N_{\text{occ}}} X_{ik}^{-1} R_{kj}, \quad i = 1, \dots, N_{\text{occ}}, \quad j = 1, \dots, N_s, \quad (15)$$

where

$$X_{ik} = \sum_{l=1}^{N_{\text{occ}}} (RQ)_{il} \tilde{P}_{S,lk}, \quad i, k = 1, \dots, N_{\text{occ}}. \quad (16)$$

Eqs. (14), (15), and (16) are derived in Appendix A. The matrix elements of P and P^{-1} that do not appear in Eqs. (14) and (15) do not contribute to observables and may be set to zero.

Canonical expectation values of one-body observables can now be computed from Eqs. (7-9) using only the N_{occ} eigenvalues $\tilde{\lambda}_i$. Because the single-particle model space is reduced to N_{occ} states, the number of terms in the Fourier sums in Eqs. (7-9) is also reduced to N_{occ} with quadrature points $\varphi_m = 2\pi m/N_{\text{occ}}$ for $m = 1, \dots, N_{\text{occ}}$, and the number of factors in Eq. (7) is reduced to N_{occ} . Grand-canonical expectation values of one-body observables can be also be computed in terms of $\tilde{\lambda}_i$ alone (using formulas obtained by simply taking only one term in the Fourier sums).

Fig. 2 compares the time spent diagonalizing the matrix S (obtained from the single-particle propagator U by a similarity transformation $S = Q^{-1}UQ$) in the full single-particle model space with the time required to diagonalize \tilde{S} in the reduced space for canonical-ensemble calculations of the the same system considered in Fig. 1. Without the reduction, the number of operations needed to diagonalize S during an update of all auxiliary fields is $O(N_t N_s^3)$, where $N_s = N_L^3$, and dominates the computational effort of the simulation. With the reduction, the number of operations is $O(N_t N_s N_{\text{occ}}^2)$, and the time spent in diagonalization for the larger lattice sizes is reduced by several orders of magnitude. The number of operations is similarly reduced from $O(N_t N_s^3)$ to $O(N_t N_s N_{\text{occ}}^2)$ in the grand-canonical ensemble.

Fig. 3 compares the total time required to compute a single sample, including five decorrelation sweeps and the calculation of observables, with and without the reduction in the single-particle model space. For the largest lattice shown the time per sample is reduced by approximately two orders of magnitude.

The code used for the figures was implemented using MPI + OpenMP parallel processing and Intel MKL routines for matrix operations, with each MPI

³The matrices P and Λ (where $\Lambda_{ij} = \lambda_i \delta_{ij}$) in the eigenvalue decomposition of U_{occ} are different from those in the eigenvalue decomposition of U in Sec. 1.2, but we use the same notation for simplicity.

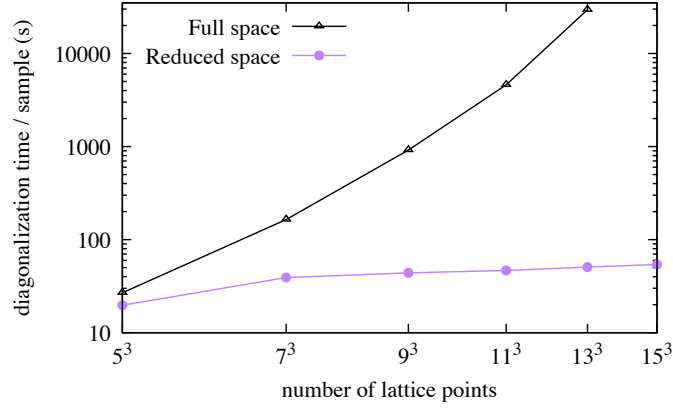


Figure 2: Time (in seconds) required to diagonalize the original matrix S of dimension N_s (triangles) and the matrix \tilde{S} of reduced dimension N_{occ} (circles) vs. the number of lattice points. Results are shown on a log-log scale for the same system as in Fig. 1.

task corresponding to an independent Monte Carlo walk. For the calculations shown, 8 OpenMP threads were used for each MPI task, and the code was run on the Intel Knight's Landing multicore architecture.

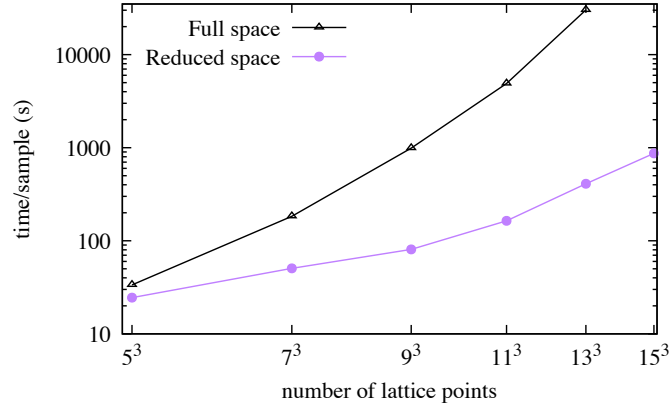


Figure 3: Time (in seconds) per sample on a log-log scale using the complete and reduced-dimension single-particle spaces for the same system as in Fig. 1. Each sample included five decorrelation sweeps and includes the calculation of observables (total energy and heat capacity).

2.2. Error estimates

In this section, we estimate the error that results from omitting the (mostly) unoccupied single-particle states. The grand-canonical partition function $Z =$

$\det(I + U) = \det(I + U_{\text{occ}} + E)$ can be expanded in E as

$$\det(I + U_{\text{occ}} + E) = \det(I + U_{\text{occ}}) + \det(I + U_{\text{occ}}) \text{tr}[(I + U_{\text{occ}})^{-1} E] + O(E^2)$$

Hence the relative error $|Z - Z_{\text{occ}}|/|Z|$ in the partition function (where $Z_{\text{occ}} \equiv \det(I + U_{\text{occ}})$) is given by

$$(Z - Z_{\text{occ}})/Z \approx \text{tr}[(I - \rho_{\text{occ}})E], \quad (17)$$

where ρ_{occ} is defined similarly to (3) but with U_{occ} replacing U . The expectation value of a one-body observable $\hat{\mathcal{O}}$ computed using U_{occ} acquires an error

$$\langle \hat{\mathcal{O}} \rangle_{\sigma} - \langle \hat{\mathcal{O}} \rangle_{\sigma, \text{occ}} = \text{tr}[\mathcal{O}(\rho - \rho_{\text{occ}})]. \quad (18)$$

Expanding

$$(I + U_{\text{occ}} + E)^{-1} = (I + U_{\text{occ}})^{-1} - (I + U_{\text{occ}})^{-1} E (I + U_{\text{occ}})^{-1} + O(E^2),$$

we find the error in the one-body density ρ to

$$\rho - \rho_{\text{occ}} \approx (I - \rho_{\text{occ}}) E (I - \rho_{\text{occ}}). \quad (19)$$

A general two-body observable $\hat{Y} = \sum_{ijkl} Y_{ijkl} a_i^{\dagger} a_j^{\dagger} a_l a_k$ is characterized by $O(N_s^4)$ non-zero matrix elements, and its expectation value can have a larger error than that of one-body observables. However, many two-body observables have only $O(N_s)$ or $O(N_s^2)$ nonzero matrix elements. For the observables we have considered in the example of the unitary Fermi gas, we find that the relative error at a given sample is still generally of order ε .

If μ_C is determined to approximately give the desired number of particles, the corresponding grand-canonical quantities approximate sufficiently well the canonical expectation values so that the above error estimates also apply for canonical-ensemble observables. At very low temperatures, however, the spectrum λ_i can have a step-like behavior, i.e., there is a well-defined Fermi energy, and after the canonical projection, eigenvalues just above the Fermi energy do contribute to observables. For this reason one should include a certain number of states above the Fermi energy, regardless of ε .

Table 1 shows the maximum error in Z_N and $\langle \hat{H} \rangle_{\sigma}$ that results from the truncation of the single-particle space for the unitary Fermi gas near the phase transition temperature, using the same parameters as in Fig. 1. We find that the sample-by-sample relative error in Z , and appropriately scaled sample-by-sample absolute error in observables, are of the same order of magnitude as the input parameter ε .

3. Field updates

To efficiently iterate through and update all time slices $t = 1, \dots, N_t$, we apply a QR decomposition only every K time slices, while still performing a

lattice	Z_N (relative)	$\langle \hat{H} \rangle_\sigma$ (absolute)	$\langle \hat{H} \rangle_\sigma$ (scaled)
5^3	6.3×10^{-8}	1.8×10^{-6}	2.6×10^{-8}
7^3	1.6×10^{-7}	3.4×10^{-6}	5.6×10^{-8}
9^3	1.3×10^{-7}	4.1×10^{-6}	6.7×10^{-8}
11^3	1.6×10^{-7}	4.0×10^{-6}	6.7×10^{-8}

Table 1: Errors in the partition function Z_N and energy $\langle \hat{H} \rangle_\sigma$ due to truncation of the single-particle model space. The errors are computed by performing two separate AFMC calculations, one using the complete model space, and the other using the model space truncation with $\varepsilon = 10^{-6}$. All other parameters are the same as in Fig. 1. The Z_N (relative) column lists the maximum relative error $\max_i |Z_N^{(i)} - Z_N^{(i)}(\varepsilon)|/|Z_N^{(i)}|$ for all complete updates of the auxiliary fields $i = 1, \dots, N_{\text{samp}} N_{\text{sweep}}$. The $\langle \hat{H} \rangle_\sigma$ (absolute) column lists the maximum absolute error in the energy for all samples, $\max_n |\langle \hat{H} \rangle_{\sigma_n} - \langle \hat{H} \rangle_{\sigma_n}(\varepsilon)|$ for $n = 1, \dots, N_{\text{samp}}$. The $\langle \hat{H} \rangle_\sigma$ (scaled) column lists the value of the $\langle \hat{H} \rangle$ (absolute) column divided by the final expectation $\langle \hat{H} \rangle$ computed from all samples.

Metropolis update at each time slice. One can avoid computing the product of two QDR decompositions at each imaginary time by observing that the factors $U_{N_t} \cdots U_1$ can be cyclically permuted while preserving the partition function.

When updating time slice t within the block $(n-1)K+1 \leq t \leq nK$, the factors in the propagator are grouped as

$$\begin{aligned} U &= (U_{N_t} \cdots U_{nK+1}) (U_{nK} \cdots U_t \cdots U_{(n-1)K+1}) (U_{(n-1)K} \cdots U_1) \\ &= (QDR)_{n+1} (U_{nK} \cdots U_t \cdots U_{(n-1)K+1}) (QDR)_{n-1}, \end{aligned} \quad (20)$$

where $(QDR)_{n+1} = U_{N_t} \cdots U_{nK+1}$ and $(QDR)_{n-1} = U_{(n-1)K} \cdots U_1$. U is related by a similarity transformation to

$$T \equiv U_t \cdots U_{(n-1)K+1} (QDR)_{n-1} (QDR)_{n+1} U_{nK} \cdots U_{t+1} \quad (21)$$

which conveniently locates U_t as the leftmost factor.

Prior to updating the fields for time slices $t = (n-1)K+1, \dots, nK$, we first compute a decomposition $QDR = (QDR)_{n-1} (QDR)_{n+1}$ and compute and cache the partial products $RU_{nK} \cdots U_t$ for $t = (n-1)K+2, \dots, nK$. We then successively update the fields for $t = (n-1)K+1, \dots, nK$ by accumulating new time slices on the left of the product (21) and removing old time slices on the right of this product using the pre-computed partial products, obtaining for each t

$$T = ADB = (U_t \cdots U_{(n-1)K+1} Q) D (RU_{nK} \cdots U_{t+1}). \quad (22)$$

The method of Sec. 2 is used to compute the partition function at time slice t using the decomposition ADB , where A and B are general complex matrices.

With this algorithm, QR decompositions are computed only every K time slices, at the cost computing extra applications of time slices. Multiplying by a factor U_t requires $O(N_s^2 \log N_s)$ operations using a fast Fourier transform, if the interaction is local in coordinate space.

Including the major operations, the complexity of the field updates is

$$O(N_t N_s^2) + O(N_t N_s N_{\text{occ}}^2) + O(N_t N_s^2 \log(N_s)) + O((N_t/K) N_s^3), \quad (23)$$

where the first term is from determining N_{occ} , the second term is from computing the partition function, the third term is from constructing the time slices, and the fourth term is from the QR decomposition. The benefit of the truncation is to replace the $O(N_t N_s^3)$ complexity of computing the partition function in the complete model space with $O(N_t N_s N_{\text{occ}}^2)$.

4. Two-body observables

The expectation value of a two-body observable can be computed from the two-body density matrix $\langle a_i^\dagger a_j a_k^\dagger a_l \rangle_\sigma$. In the grand-canonical ensemble, this can be computed from the one-body densities using Wick's theorem

$$\langle a_i^\dagger a_j a_k^\dagger a_l \rangle_\sigma = \langle a_i^\dagger a_j \rangle_\sigma \langle a_k^\dagger a_l \rangle_\sigma + \langle a_i^\dagger a_l \rangle_\sigma (\delta_{k,j} - \langle a_k^\dagger a_j \rangle_\sigma).$$

In the canonical ensemble

$$\langle a_i^\dagger a_j a_k^\dagger a_l \rangle_\sigma = \frac{e^{-\beta\mu}}{Z_N N_s} \sum_{m=1}^{N_s} e^{-i\varphi_m N} \langle a_i^\dagger a_j a_k^\dagger a_l \rangle_\sigma^{(m)} \eta_m \quad (24)$$

where

$$\langle a_i^\dagger a_j a_k^\dagger a_l \rangle_\sigma^{(m)} = \gamma_{ji}^{(m)} \gamma_{lk}^{(m)} + \gamma_{li}^{(m)} (\delta_{kj} - \gamma_{jk}^{(m)}), \quad (25)$$

and $\gamma_{ij}^{(m)} \equiv \langle a_j^\dagger a_i \rangle_\sigma^{(m)}$ are given in Sec. 1.2.

In the special case of the two-species cold atom system, in which atoms of the same species do not interact, the two-body canonical-ensemble density matrix of interest factorizes and is simple to compute, i.e., $\langle a_{i\uparrow}^\dagger a_{j\uparrow} a_{k\downarrow}^\dagger a_{l\downarrow} \rangle_\sigma = \langle a_{i\uparrow}^\dagger a_{j\uparrow} \rangle_\sigma \langle a_{k\downarrow}^\dagger a_{l\downarrow} \rangle_\sigma$. This relies on the factorization of the propagator into different species, $\hat{U} = \hat{U}_\uparrow \hat{U}_\downarrow$ for each auxiliary-field configuration σ . However, in general this is not the case.

For an observable which requires the evaluation of all elements $\langle a_i^\dagger a_j a_k^\dagger a_l \rangle_\sigma$, it is difficult to obtain a scaling even of $O(N_s^4)$, since the calculation of each element with indices i, j, k, l typically requires at least one computational loop.

It is convenient to first compute the matrices $\gamma_{ij}^{(m)}$ and then use these in the calculation of the observables. Using the eigenvalue decomposition of U_{occ} , we have

$$\gamma_{ij}^{(m)} = \sum_{\alpha=1}^{N_{\text{occ}}} P_{i\alpha} (1 + \tilde{\lambda}_\alpha^{-1} e^{-\beta\mu_C} e^{-i\varphi_m})^{-1} P_{\alpha j}^{-1}, \quad (26)$$

where $\varphi_m = 2\pi m/N_{\text{occ}}$ for $m = 1, \dots, N_{\text{occ}}$. Computing all N_{occ} γ matrices in Eq. (26) requires $O(N_s^2 N_{\text{occ}}^2)$ operations and $O(N_s^2 N_{\text{occ}})$ memory. Without the model space truncation, this calculation requires $O(N_s^4)$ floating-point operations and $O(N_s^3)$ memory, both of which become prohibitive for large N_s .

The computational effort and memory required can be reduced further by minimizing the number of quadrature points used in the Fourier sum. To accomplish this we extend an idea introduced in Ref. [20] and used in Ref. [21]. For a given number of quadrature points N_{FT} in the Fourier sum, we have the identity

$$\frac{1}{N_{\text{FT}}} \sum_{m=1}^{N_{\text{FT}}} e^{i\varphi_m(N-N')} = \begin{cases} 1, & N = N' \pmod{N_{\text{FT}}} \\ 0, & \text{otherwise} \end{cases},$$

where $\varphi_m = 2\pi m/N_{\text{FT}}$. Using N_{FT} quadrature points to calculate the canonical partition function, we obtain

$$\begin{aligned} Z_N(N_{\text{FT}}) &\equiv \frac{e^{-\beta\mu_C N}}{N_{\text{FT}}} \sum_{m=1}^{N_{\text{FT}}} e^{-i\varphi_m N} \text{Tr}(e^{i\varphi_m \hat{N}} e^{\beta\mu_C \hat{N}} \hat{U}) \\ &= \sum_{k=0, \pm 1, \dots} \text{Tr}_{N+kN_{\text{FT}}}(\hat{U} e^{\beta\mu_C(\hat{N}-N)}). \end{aligned} \quad (27)$$

The reduced number of quadrature points therefore includes contributions from particle numbers N , $N \pm N_{\text{FT}}$, $N \pm 2N_{\text{FT}}$, \dots . With μ_C chosen to give $\langle \hat{N} \rangle_\sigma \approx N$, the largest term on the r.h.s of Eq. (27) is the N -particle trace, with the $N \pm N_{\text{FT}}$, $N \pm 2N_{\text{FT}}$, \dots traces giving increasingly smaller corrections.

Given a desired error tolerance ε for the particle-number projection, we can determine the minimal necessary value of N_{FT} by starting with a small value of N_{FT} and computing the partition function Z_N and diagonal one-body densities ρ_α for increasingly large values of N_{FT} until the conditions

$$|\log Z_N - \log Z_N(N_{\text{FT}})| < \varepsilon,$$

$$\sum_{\alpha} |\rho_\alpha - \rho_\alpha(N_{\text{FT}})| < \varepsilon,$$

are both satisfied. Although this N_{FT} is determined by the one-body densities, it can in practice be effectively used also for two-body observables. Using this algorithm, the calculation of the $\gamma_{ij}^{(m)}$ matrices in Eq. (26) requires $O(N_s^2 N_{\text{occ}} N_{\text{FT}})$ operations and $O(N_s^2 N_{\text{FT}})$ memory.

The contributions from fully occupied states with $(1 + \tilde{\lambda}_\alpha^{-1} e^{-i\varphi_m})^{-1} \approx 1$ in Eq. (26) are independent of m , and thus can be calculated separately, offering an additional optimization.

Fig. 4 shows a comparison of the time required to compute all of the matrices $\gamma_{ij}^{(m)}$ with and without the truncation in the size of the single-particle model space and the reduction in the number of points N_{FT} in the Fourier transform of the particle-number projection. Here we used a single particle-number projection onto the total number of particles $N = 66$, as done for our calculations for the spin susceptibility in Ref. [1]. We find $N_{\text{FT}} \approx 14$, independent of the lattice size. The results in Fig. 4 (shown on a log-log scale) confirms the reduction of the $O(N_s^3)$ scaling (slope of ≈ 3) when using the full single-particle model space to $O(N_s^2)$ when using the reduced model space (slope of ≈ 2).

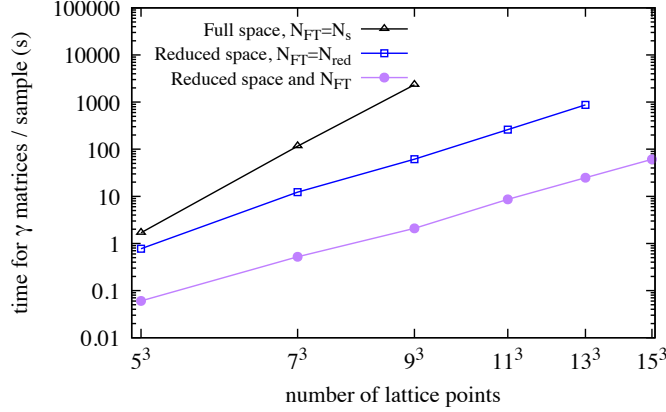


Figure 4: Comparison of the time required to compute all of the matrices $\gamma_{ij}^{(m)}$, on a log-log scale. The parameters of the calculation are as in Fig. 1, except that only one particle-number projection onto the total number of particles $N = 66$ is used. Black triangles show the time required using the complete model space of N_s single-particle states and N_s terms in the Fourier transform of the canonical projection. The curve is approximately linear with a slope of ≈ 4 , confirming the $O(N_s^4)$ scaling of the usual two-body canonical projection. Blue squares show the time required using the reduced model space of N_{occ} states and $N_{FT} = N_{occ}$ terms in the Fourier transform. Purple dots show the time required using the reduced model space of N_{occ} states and a minimal number of points in the Fourier transform ($N_{FT} \approx 14$). The slope of the later two curves is ≈ 2 , confirming the reduced $O(N_s^2)$ scaling (note that N_{occ} is approximately constant).

5. Conclusion

Finite-temperature auxiliary-field quantum Monte Carlo (AFMC) calculations typically have a computational scaling of $O(N_s^3)$ or higher power in N_s , where N_s is the number of single-particle states. We introduced a major improvement which reduces this scaling by eliminating the (mostly) unoccupied states from the calculation of the partition function and observables at any given configuration of the auxiliary fields. Since the single-particle states must be periodically re-orthogonalized as the single-particle propagator $\hat{U}(\sigma)$ is applied, this produces a decomposition (such as the *QDR* decomposition), which allows us to identify and eliminate the (mostly) unoccupied states. The remaining model space has a reduced dimension N_{occ} of the significantly occupied states, which scales gently with the number of particles N and is usually of the order N . Our method is applicable in both canonical ensemble and grand-canonical ensemble calculations. The speedup of our algorithm is particularly substantial in systems with $N \ll N_s$.

For the canonical ensemble, the calculation of general two-body observables in the reduced model space still requires the calculation of N_{occ} matrices of dimension N_s . We have introduced a method that further reduces the required number of these matrices, greatly reducing the computational effort for two-

body observables.

These improvements can enable otherwise impractical studies of dilute fermionic systems. In particular, we have used these methods to carry out finite-temperature lattice AFMC calculations for the spin-balanced unitary Fermi gas (where N_s is proportional to the cubic power of the linear size of the lattice), including precision studies of the pseudogap phenomenon [1, 2], and of thermodynamic observables in the continuum limit [3].

The remaining $O(N_s^3)$ dependence in the algorithm exists only in the calculation of the QR decomposition, with a scaling of $O((N_t/K)N_s^3)$. This can also be addressed by performing the single-particle model-space reduction within the QR decomposition itself, as was done in Ref. [4].

Acknowledgments

This work was supported in part by the U.S. DOE grants Nos. DE-SC0019521, DE-FG02-91ER40608, and DE-FG02-00ER41132. The research presented here used resources of the National Energy Research Scientific Computing Center, which is supported by the Office of Science of the U.S. Department of Energy under Contract No. DE-AC02-05CH11231. We also thank the Yale Center for Research Computing for guidance and use of the research computing infrastructure.

Appendix A

In this Appendix we discuss how to obtain the eigenvectors and eigenvalues of S_{occ} from those of the truncated matrix \tilde{S} .

Consider a nonzero eigenvalue λ of S_{occ} . If $S_{\text{occ}} \mathbf{y} = \lambda \mathbf{y}$, then since the last $N_s - N_{\text{occ}}$ rows of S_{occ} are zero, so are the corresponding entries of $\lambda \mathbf{y}$. If $\lambda \neq 0$, this means the last $N_s - N_{\text{occ}}$ entries of \mathbf{y} are zero. Hence all right eigenvectors of S_{occ} with $\lambda \neq 0$ have the form

$$\mathbf{y} = \begin{pmatrix} y_1 \\ \vdots \\ y_{N_{\text{occ}}} \\ 0 \\ \vdots \end{pmatrix}, \quad (\lambda \neq 0).$$

i.e., are contained in the subspace $V_{N_{\text{occ}}} = \text{sp}\{\mathbf{e}_1, \dots, \mathbf{e}_{N_{\text{occ}}}\}$ spanned by the first N_{occ} unit vectors \mathbf{e}_i . Since S_{occ} maps this space onto itself, $S_{\text{occ}} : V_{N_{\text{occ}}} \rightarrow V_{N_{\text{occ}}}$, one can obtain all right eigenvectors with $\lambda \neq 0$ by diagonalizing S_{occ} in this subspace. The matrix of S_{occ} in this subspace is the $N_{\text{occ}} \times N_{\text{occ}}$ matrix \tilde{S} .

Any right eigenvector of \tilde{S} therefore corresponds to a right eigenvector of S_{occ} , obtained by appending zeros. The other right eigenvectors of S_{occ} have

$\lambda = 0$ and are exactly the elements of the nullspace of S_{occ} . Since the last $N_s - N_{\text{occ}}$ rows of S_{occ} are zero, the nullspace is

$$\text{Null}(S_{\text{occ}}) = \{\mathbf{x} \in V | \mathbf{x} \text{ is orthogonal to the first } N_{\text{occ}} \text{ rows of } S_{\text{occ}}\}. \quad (28)$$

Note generally $\text{Null}(S_{\text{occ}}) \neq \text{sp}\{\mathbf{e}_{N_{\text{occ}}+1}, \dots, \mathbf{e}_{N_s}\}$. So the transformation matrix has the form

$$P_S = \left(\begin{array}{c|c|c|c|c} | & & | & | & \\ \mathbf{y}_1 & \dots & \mathbf{y}_{N_{\text{occ}}} & \mathbf{n}_1 & \dots \\ | & & | & | & \end{array} \right) = \left(\begin{array}{c|c} \tilde{P}_S & \text{Basis for} \\ \hline 0 & \text{Null}(S_{\text{occ}}) \\ 0 & \end{array} \right),$$

where \tilde{P}_S is the matrix whose columns are the eigenvectors of \tilde{S} . We need only the first N_{occ} columns of P for computing the density matrix.

We also require the first N_{occ} rows of the inverse, i.e., the matrix whose rows are the left eigenvectors \mathbf{w}_i of S_{occ} . This will have the form

$$P_S^{-1} = \left(\begin{array}{c|c|c} \text{---} & \mathbf{w}_1 & \text{---} \\ & \vdots & \\ \text{---} & \mathbf{w}_{N_{\text{occ}}} & \text{---} \\ & \vdots & \end{array} \right) = \left(\begin{array}{c|c} \tilde{P}_S^{-1} & A \\ \hline x & x & x & x & x \\ x & x & x & x & x \end{array} \right).$$

The row vectors \mathbf{w}_i for $i = 1, \dots, N_{\text{occ}}$ are determined by the condition $P_S P_S^{-1} = I$, i.e.,

$$\mathbf{w}_i \cdot \mathbf{y}_j = \delta_{i,j}, \quad \mathbf{w}_i \cdot \mathbf{n}_k = 0 \quad (i, j = 1, \dots, N_{\text{occ}}; \text{all } k), \quad (29)$$

where \mathbf{n}_k , $k = 1, \dots, N_s - N_{\text{occ}}$ is any basis for $\text{Null}(S_{\text{occ}})$. The first N_{occ} entries of the vector \mathbf{w}_i are the entries in the i th row of \tilde{P}_S^{-1} , since one has the identity $\tilde{P}_S^{-1} \tilde{P}_S = I$ for the block sub-matrices $\tilde{P}_S, \tilde{P}_S^{-1}$. However, the remaining $N_s - N_{\text{occ}}$ entries are generally nonzero so that \mathbf{w}_i can be orthogonal to all of the \mathbf{n}_k . These entries comprise the submatrix A , which is unknown and must be determined.

To determine A , consider that since \mathbf{w}_i must be orthogonal to the nullspace of S_{occ} , by Eq. (28) it is contained in the span of the first N_{occ} rows \mathbf{r}_k of RQ . We can write

$$\mathbf{w}_i = \sum_{k=1}^{N_{\text{occ}}} B_{ik} \mathbf{r}_k, \quad (30)$$

for some coefficients B_{ik} . Then the first part of condition (29) becomes

$$\mathbf{w}_i \cdot \mathbf{y}_j = \sum_{k=1}^{N_{\text{occ}}} B_{ik} \mathbf{r}_k \cdot \mathbf{y}_j = \delta_{ij},$$

so we obtain

$$B_{ik} = X_{ik}^{-1} \quad \text{where} \quad X_{ik} \equiv \mathbf{r}_i \cdot \mathbf{y}_k.$$

The first N_{occ} rows of P_S^{-1} can therefore be obtained by inverting the $N_{\text{occ}} \times N_{\text{occ}}$ matrix X and forming the linear combinations (30). In terms of matrix operations,

$$P_{S,ij}^{-1} = \sum_{k=1}^{N_{\text{occ}}} X_{ik}^{-1} (RQ)_{kj}, \quad X_{ik} = \sum_{l=1}^{N_{\text{occ}}} (RQ)_{il} P_{S,lk}, \quad (31)$$

where $i, k = 1, \dots, N_{\text{occ}}$ and $j = 1, \dots, N_s$.

Now, to obtain the eigenvalue decomposition $U_{\text{occ}} = P\Lambda P^{-1}$, we observe that $U_{\text{occ}} = QS_{\text{occ}}Q^{-1} = (QP_S)\Lambda(P_S^{-1}Q^{-1})$, and obtain

$$P_{ij} = \sum_{k=1}^{N_{\text{occ}}} Q_{ik} \tilde{P}_{S,kj}, \quad i = 1, \dots, N_s, \quad j = 1, \dots, N_{\text{occ}} \quad (32)$$

$$P_{ij}^{-1} = \sum_{k=1}^{N_{\text{occ}}} X_{ik}^{-1} R_{kj}, \quad i = 1, \dots, N_{\text{occ}}, \quad j = 1, \dots, N_s \quad (33)$$

where Eqs. (32) and (33) specify only the indices i, j which contribute to observables. The other matrix elements may be set to zero.

References

- [1] S. Jensen, C. N. Gilbreth, and Y. Alhassid, *Nature of pairing correlations in the homogeneous fermi gas at unitarity* (2018), [1801.06163](#).
- [2] S. Jensen, C. N. Gilbreth, and Y. Alhassid, *Eur Phys J Spec Top* **227**, 2241 (2019).
- [3] S. Jensen, C. N. Gilbreth, and Y. Alhassid, *The contact in the unitary fermi gas across the superfluid phase transition* (2019), [1906.10117](#).
- [4] Y.-Y. He, H. Shi, and S. Zhang, *Reaching the continuum limit in finite-temperature ab initio field-theory computations in many-fermion systems* (2019), [arXiv:1906.02247](#).
- [5] S. Koonin, D. Dean, and K. Langanke, *Phys. Rep.* **278**, 2 (1997), ISSN 0370-1573.
- [6] Y. Alhassid, *Int. J. Mod. Phys. B* **15**, 1447 (2001).
- [7] Y. Alhassid, in *Emergent Phenomena in Atomic Nuclei from Large-Scale Modeling: a Symmetry-Guided Perspective*, edited by K. D. Launey (World Scientific, Singapore, 2017), pp. 267–298.
- [8] J. Hubbard, *Phys. Rev. Lett.* **3**, 77 (1959).
- [9] R. Stratonovich, *Dokl. Akad. Nauk. S.S.S.R.* **115**, 1097 (1957), [*Sov. Phys. Dokl.* **2**, 416 (1957)].

- [10] S. Beyl, F. Goth, and F. F. Assaad, Phys. Rev. B **97**, 085144 (2018).
- [11] S. Duane, A. Kennedy, B. J. Pendleton, and D. Roweth, Physics Letters B **195**, 216 (1987), ISSN 0370-2693.
- [12] W. E. Ormand, D. J. Dean, C. W. Johnson, G. H. Lang, and S. E. Koonin, Phys. Rev. C **49**, 1422 (1994).
- [13] S. Rombouts and K. Heyde, Journal of Computational Physics **140**, 453 (1998), ISSN 0021-9991.
- [14] R. Rehman and I. C. F. Ipsen, *La budde's method for computing characteristic polynomials* (2011), [1104.3769](#).
- [15] Z. Wang, F. F. Assaad, and F. Parisen Toldin, Phys. Rev. E **96**, 042131 (2017).
- [16] Shill, C.R. and Drut, J.E., EPJ Web Conf. **175**, 03003 (2018).
- [17] C. Gilbreth and Y. Alhassid, Computer Physics Communications **188**, 1 (2015), ISSN 0010-4655.
- [18] E. Y. Loh Jr and J. E. Gubernatis, in *Electronic phase transitions (Modern Problems in Condensed Matter Sciences)*, edited by W. Hanke and Y. Kopaev (North-Holland, 1992), pp. 177–235.
- [19] Z. Bai, C. Lee, R.-C. Li, and S. Xu, Linear Algebra Appl. **435**, 659 (2011), ISSN 0024-3795.
- [20] L. Fang, Ph.D. thesis, Yale University (2005).
- [21] Y. Alhassid, L. Fang, and H. Nakada, Phys. Rev. Lett. **101**, 082501 (2008).